Commun. Comput. Chem.
doi: 10.4208/cicc.2013.v1.n1.7

Vol.**1**, No.1, pp. 63-71
January 2013

REGULAR ARTICLE

Five New Ab initio Potential Energy Surfaces for the $O(^3P, ^1D) + H_2$ System

Pei-Yu Zhang[1,*] and Shuang-Jiang Lv[1]

[1] *State Key Laboratory of Molecular Reaction Dynamics, Dalian Institute of Chemical Physics, Chinese Academy of Sciences, Dalian 116023, China*

Received 20 December 2012; Accepted (in revised version) 17 January 2013

Special Issue: Guo-Zhong He Festschrift

Abstract: Five new potential energy surfaces ($1^{1,3}$A', 2^1A', $1^{1,3}$A'') for O (^3P, ^1D) + H_2 system have been constructed. The *ab intio* single-point energies were calculated for 11060 geometries using five-state state-averaged complete active space self-consistent field (SA-CASSCF) and Davidson corrected multireference configuration interaction method (MRCI+Q) with aug-cc-pVQZ basis sets. A back–propagation neural network (NN) is utilized to fit the potential energy surfaces. The fitted potential surfaces and some important crossings among them are presented. Adiabatic quantum scattering calculations with total angular momentum $J = 0$ are carried out on the new potential surfaces and compared with the results based on previous surfaces.

AMS subject classifications: 70F07, 74J20

Key words: Potential energy surfaces, O + H_2 reaction, Ab initio calculation

1 Introduction

Reaction of O with H_2 has been the project of study for many years. This reaction has generated considerable interest for a variety of nonadiabatic phenomenon: nonadiabatic transition of singlet states [1-3], spin-orbit induced triplet-singlet transition [4] and transition

* Corresponding author. *Email address*: pyzhang@dicp.ac.cn (P. –Y. Zhang)

in exit-channel region for studying multiplet branching between OH($X^2\Pi$) multiplet levels [5]. Thus, several potential energy surfaces [1,6,7,8,9] have been developed to study adiabatic and nonadiabatic reaction dynamics.

There are eight potential energy surfaces (PESs) accessible to reactants O (^3P, ^1D) + H_2: 1-3^{1}A', 1, 2^{1}A'', 1, 2^{3}A'', 1^{3}A'. Four states (1^{1,3}A', 1^{1,3}A'') of them correspond to ground products H + OH ($X^2\Pi$), 2^{1}A' correlates with excited products H + OH($A^2\Sigma$), and the other three excited states(3^{1}A', 2^{1}A'', 2^{3}A'') are repulsive and correlate with upper excited products. High-quality PESs have been obtained for ground state 1^{1}A'[7-9]. Dobbyn and Knowles [1] have constructed DK PESs of singlet states (1,2^{1}A', 1^{1}A'') along with electrostatic coupling between 1^{1}A' and 2^{1}A'. And many nonadiabatic dynamics calculations have been carried out on DK PESs [2,3,10,11]. The above singlet PES 1^{1}A', and triplet PESs 1^{3}A'', 1^{3}A' of Rogers *et al*.[6] were used to study spin-orbit induced transition [12-14]. There is no degeneracy in asymptote OH-H region of the above triplet states, where switching function was used to correct this inadequacy. Recently, Alexander *et al*.[5] have carried out *ab initio* calculations for the four states (1^{1,3}A', 1^{1,3}A'') in product region to study multiplet branching in O(^1D) + H_2 reaction. Nonadiabatic reaction dynamics requires accurate representations of the *ab initio* PESs involved in reaction. The energy intervals among the coupling PESs and locations of crossing seams have a big effect on transition probabilities, which should be determined accurately. There is a clearly need for removing unnecessary error from different *ab initio* method and fitting procedures for PESs involved in those nonadiabatic dynamics. For this reason, in this paper new high-quality potential surfaces were constructed employing a SA-CASSCF/MRCI+Q scheme with the same weight given to all of the states in state-average procedure.

In this work, we developed five global potential surfaces (1, 2^{1}A', 1^{1}A'', 1^{3}A'' and 1^{3}A') correlate with reactants O(^3P, ^1D) + H_2 and products H + OH($X^2\Pi$, $A^2\Sigma$). The PESs are directly constructed by *ab initio* energies without considering spin-orbit and electrostatic coupling. The paper is organized as follows. In the next section, *ab initio* molecular electronic structure theory is outlined with stationary point properties for the states, and the fitting procedure of PESs is presented in detail. In Section 3, several features of the surfaces are discussed. Conclusions are given in Section 4.

2 Methods

The energies for all data points were calculated using multi-reference configuration interaction (MRCI) scheme with Dunning's aug-cc-pVQZ atomic orbital basis set [15]. Multireference Davidson correction was included to account for the effect of higher-order

correlation. The MRCI+Q calculations were based on state-averaged CASSCF (SA-CASSCF) method, and equal weights were assigned to each of the five states (1, 2^1A', 1^1A'', 1^3A'' and 1^3A'). The active space included orbitals of 2*a*'-8*a*', 1*a*'' and 2*a*''. The SA-CASSCF/MRCI+Q calculations were done with MOLPRO2002 code [16].

The *ab initio* points are computed on a grid in Jacobi coordinates *R*, *r*, and θ for O + H_2 atom–diatom system, which is created by *R*(in bohrs) = {0.4, 0.6, 0.8, 0.9, 1.0, 1.05, 1.1, 1.15, 1.2, 1.25, 1.3, 1.35, 1.4, 1.45, 1.5, 1.55, 1.6, 1.65, 1.7, 1.75, 1.8, 1.85, 1.9, 1.95, 2.0, 2.05, 2.1, 2.15, 2.2, 2.25, 2.3, 2.35, 2.4, 2.45, 2.5, 2.55, 2.6, 2.65, 2.7, 2.75, 2.8, 2.9, 3.0, 3.1, 3.2, 3.3, 3.4, 3.7, 4.0, 4.5, 5.0, 5.5, 6.0, 6.5, 7.0, 7.5, 8.0, 8.5, 10.0, 12.0, 15.0}, *r*(in bohrs) = {0.6, 0.8, 1.0, 1.2, 1.3, 1.4, 1.5, 1.6, 1.7, 1.8, 1.9, 2.0, 2.1, 2.2, 2.3, 2.4, 2.5, 2.6, 2.8, 3.0, 3.2, 3.4, 3.8, 4.2, 5.0, 6.0, 7.0, 8.0, 10.0} and θ(in degrees)= {0, 15, 30, 45, 60, 75, 90}.

The global PESs are fitted using Neural Networks. The function of adiabatic PESs for the reaction is written as following many-body expansion:

$$V(\mathbf{r}) = V^{(1+2)}(\mathbf{r}) + V(\mathbf{x}) \tag{1}$$

$V(\mathbf{r})^{(1+2)}$ is the one- and two-body sum and $V(\mathbf{x})$ is the rest of interaction term. Two-body potentials were represented within the reproducing kernel Hilbert space method [17]. In the procedure for construction of PESs, the primary variables **r** is vector of three internuclear distances r_i (i = 1 - 3), and the auxiliary variables **x** is vector with elements x_i = exp (- 0.5r_i). $V(\mathbf{x})$ has the commonly used analytic potential forms of single-hidden-layer Neural Network and can be written as [18]

$$V(\mathbf{x}) = \sum_{p=1}^{n} c_p (1 + e^{\mathbf{w_p} \bullet \mathbf{x} + b_p})^{-1} \tag{2}$$

The root mean square (rms) errors are 0.58, 1.00, 0.28, 0.38 and 0.42 Kcal/mol for 1^1A', 2^1A', 1^1A'', 1^3A'' and 1^3A', respectively. After examining the fitted potential energy surfaces carefully, unphysical features have been found in asymptotic and dissociation region of O + H_2. Thus, the *ab initio* points for *R* > 3.0 bohrs are selected and fitted with rms errors of 0.28, 1.00, 0.31, 0.18 and 0.25 Kcal/mol, respectively. A switching function $f_{sw}(R)$ is employed to smoothly connect the global PESs V_{global} and PESs V_{asym} in asymptotic regions.

$$f_{sw}(R) = \frac{1.0 - \tanh(3.0(R - 3.5))}{2.0} \tag{3}$$

Switching is done following the equation

$$V = V_{global} \times f_{sw}(R) + V_{asym} \times (1.0 - f_{sw}(R)) \tag{4}$$

3 Results and discussion

The 1^1A' PES has a T-shaped minimum-energy path (MEP). **Figure 1(a-e)** displays contour plots of 1^1A', 2^1A', 1^1A'', 1^3A'' and 1^3A' fitted potential surfaces in Jacobi coordinates (R, r) for a fixed angle of θ = 90°. The configuration of water molecular corresponds to 1^1A' minimum. As seen in **Figure 1(a)**, the 1^1A' PES has minimum energy -166.87 Kcal/mol at r_{OH1} = r_{OH2} = 1.810 bohrs, ∠HOH = 103.8°, while both the corresponding *ab initio* and experimental values are -167.0 Kcal/mol. Thus the present energy surfaces can reproduce experimental values well. **Figure 1** also shows the crossings between 1^1A' and triplet PESs (1^3A'' and 1^3A'), which are important in nonadiabatic transition between singlet and triplet states induced by spin-orbital coupling. R values of crossing increase along with H_2 distance r. The crossing between 1^3A'' and 1^1A' has minimum energy (-27.52 Kcal/mol) at R = 2.83 bohrs and r = 1.52 bohrs. And the crossing between 1^3A' and 1^1A' has minimum energy (-24.47 Kcal/mol) at R = 2.88 bohrs and r = 1.50 bohrs. Potential energies of the five electronic states along 1^1A' MEP are given in **Figure 1(f)**. The A' surfaces (2^1A' and 1^3A') have high barriers and the A'' surfaces (1^3A'' and 1^1A'') are much flat along 1^1A' MEP. The heights of energy barriers are 1.59 and 70.09 Kcal/mol for 1^3A'' and 1^3A' PESs, respectively. If one is considering O (^1D) + H_2 collisions and transition from 1^1A' state to triplet states, most of products H + OH ($X^2\Pi$) are obtained on 1^3A'' state, and the products O(^3P) + H_2 rebound by the barrier of 1^3A'.

1^3A'' and 1^3A' PESs have the same linear minimum-energy paths, and 1^1A', 2^1A', 1^1A'', 1^3A'' and 1^3A' PESs for linear configurations are shown in **Figure 2(a-e)**. 1^1A' has no barrier along 1^3A'' MEP, and two other singlet PESs 2^1A' and 1^1A'' have a small barrier in O-H_2 entrance channel with barrier heights of 1.6 and 1.5 Kcal/mol, respectively. There is a potential well on 2^1A' PES, with a depth of -9.7 Kcal/mol at r_{OH} = 2.0 bohrs and r_{HH} = 1.7 bohrs. Gray *et al*. have studied nonadiabatic transition between 2^1A' and 1^1A' through conical intersections [2]. They found that the non-zero reaction probabilities originated from nonadiabatic transition even through the reactants on 2^1A' state is initiated at very low energies below the barrier of 2^1A' PES. Fig. 2(f) shows the potential energies of five electronic states along the 1^3A'' MEP. Saddle point of fitted 1^3A'' PES is found at r_{OH} = 2.28 bohrs and r_{HH} = 1.70 bohrs with barrier height of 13.27 Kcal/mol. Corresponding *ab initio* values is 13.12 Kcal/mol at r_{OH} = 2.30 bohrs and r_{HH} = 1.70 bohrs, and the difference between the fitted and *ab initio* barrier height is 0.15 Kcal/mol.

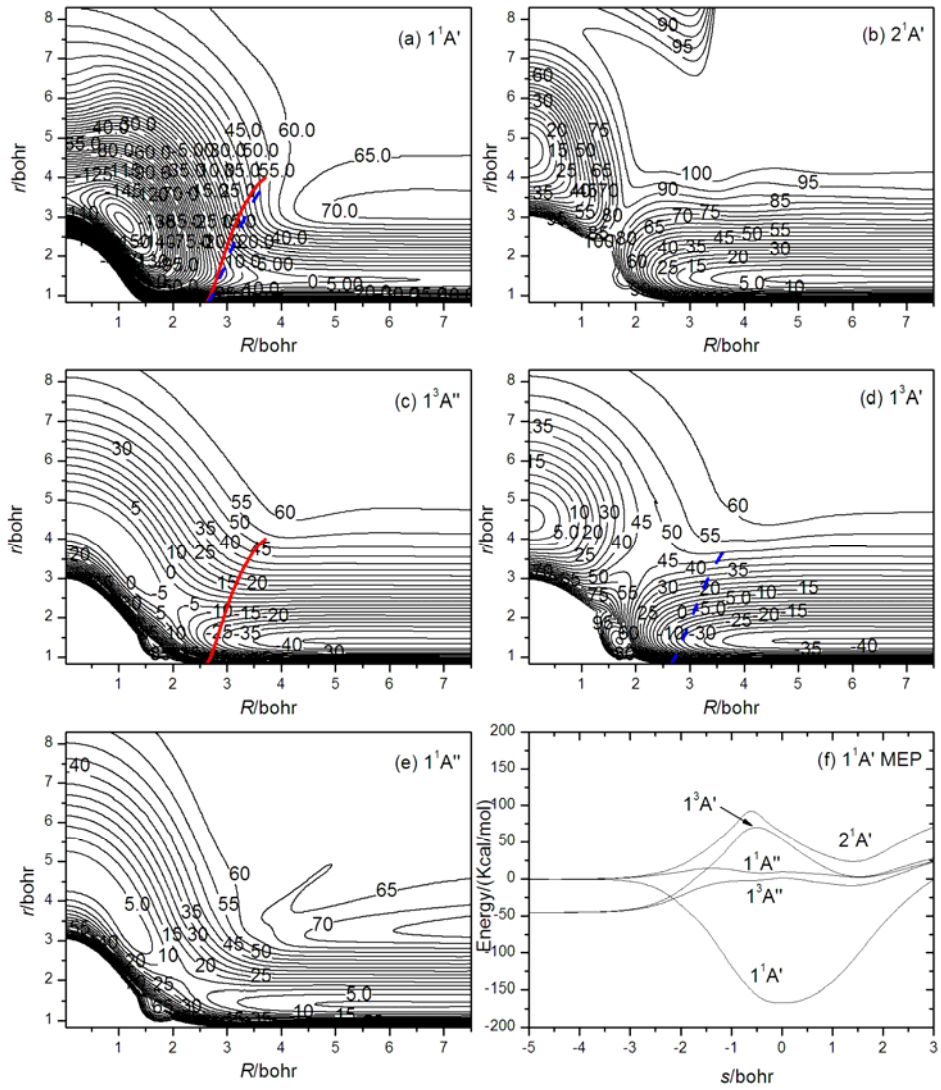

Figure 1: (a-e) Contour plots of the 1^1A', 2^1A', 1^1A'', 1^3A'' and 1^3A' potential surfaces in Jacobi coordinate (R, r) for a fixed angle of θ = 90°. Red solid line corresponds to crossing between 1^1A' and 1^3A''. Blue dashed line corresponds to crossing between 1^1A' and 1^3A'. (f) The potential energies of the five electronic states along the minimum-energy path of 1^1A' potential surface.

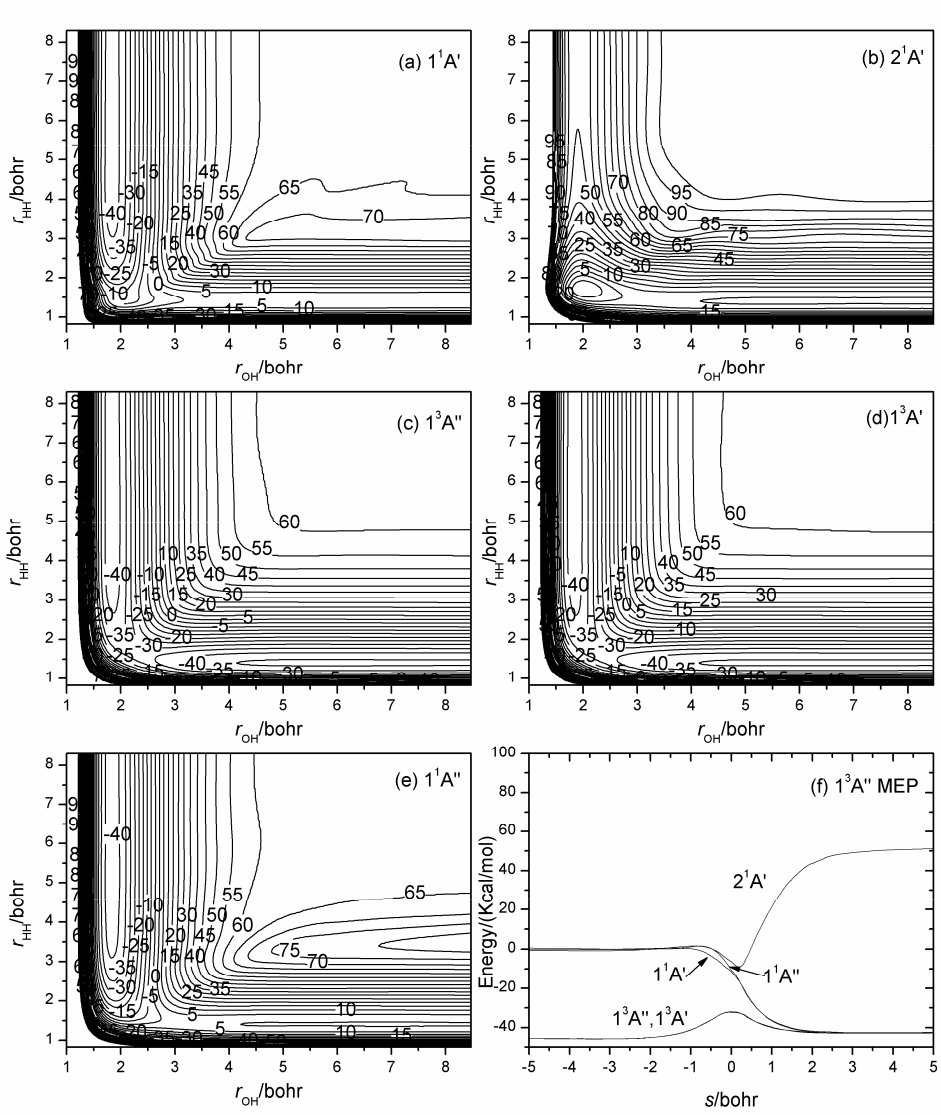

Figure 2: (a-e) Contour plots of the 1^1A', 2^1A', 1^1A'', 1^3A'' and 1^3A' potential surfaces in internal coordinate (r_{HH}, r_{OH1}, r_{OH2}) for linear configurations (r_{OH2} = r_{HH} + r_{OH1}). (f) The potential energies of the five electronic states along the minimum-energy path of 1^3A'' potential surface.

To examine the accuracy of the above surfaces, we carried out adiabatic quantum dynamics calculations with total angular momentum J = 0. The theoretical studies are based on singlet PESs (1^1A' and 1^1A'') for the reaction O(^1D) + H_2 → H + OH($X^2\Pi$) and triplet PESs

($1^3A''$ and $1^3A'$) for reaction $O(^3P) + H_2 \rightarrow H + OH(X^2\Pi)$. The $2^1A'$ correlates with excited products H + OH ($A^2\Sigma$) and is not considered for dynamics calculations. The quantum dynamics calculations are performed using the real wave-packet program developed by Gary et al. and the parameters are the same as their works [3,19]. Initial rovibrational state of H_2 is $v = j = 0$. Only the real part of wave packet is employed and propagated with Chebyshev iterations in the reactant channel. Compared with ordinary complex wave-packet quantum approaches, the time-dependent real wave-packet method decreases the computer memory requirements and improves the efficiency.

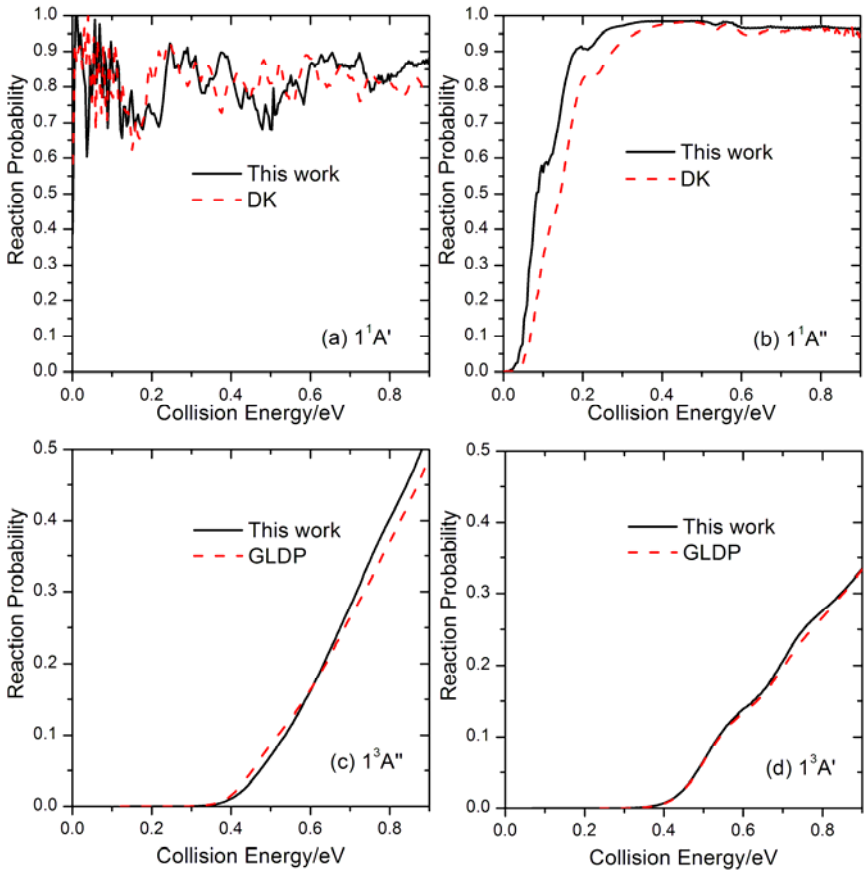

Figure 3: (a-d) Reaction probabilities for O + H_2 reaction with total angular momentum $J = 0$ on the new surfaces $1^1A'$, $1^1A''$, $1^3A'$ and $1^3A''$ PESs, respectively. The computed results on previous PESs were also showed as dashed lines [1, 6].

Figure 3 displays the computed reaction probabilities with total angular momentum $J = 0$. The computations on the new $1^1A'$ and $1^3A'$ PESs give similar quantum results as the

previous PESs (**Figure 3(a)** and **3(d)**) [1, 6]. The positions of resonances differ for the new $1^1A'$ surface and the corresponding DK surface. Further calculations of integral cross sections for the two surfaces should be carried to find the effect of different positions of resonances. In general, most oscillations of reaction probability will be smoothed by including more reaction probabilities for relevant J values. The reaction probability of new $1^3A''$ PES shown in **Figure 3(b)** is bigger than that of DK PES [1]. The barrier of new PES is 0.02 eV smaller than that of DK PES, and gives lower threshold energy. The reaction probability of new $1^3A''$ PES shown in **Figure 3(c)** is slightly smaller than the result of GLDP PES [6] at the collision energy $E_T < 0.6$ eV and the situation is opposite at $E_T > 0.6$ eV. The barrier of GLDP PES has a height of 13.04 Kcal/mol, smaller than their *ab initio* value (13.2 Kcal/mol). Thus, the GLDP gives lower reactive threshold energy. The reaction probability of $1^3A'$ state is smaller than that of $1^3A''$, which is consistent with high barrier of $1^3A'$ for T-shaped configuration shown in **Figure 1(d).**

4 Conclusions

We have calculated and fitted potential energy surfaces for the five electronic states of O(^3P, ^1D) + H_2 system. The fitted PESs are excellent in reproducing *ab initio* values of properties for saddle points. The linear and T-shaped contour maps and corresponding minimum-energy paths have been discussed in detail. The representations of resulting PESs allow for efficient evaluation of potential energies and their derivatives, and the PESs can be used to perform adiabatic/nonadiabatic semiclassical or quantum computations. With the same *ab initio* method and fitting procedures for all of five PESs, the resulting PESs provide accurate energy intervals among the coupling PESs and locations of crossing seams. Thus the present work allows us to carry further nonadiabatic quantum dynamics calculations on the title system for studying the spin-orbit and electrostatic coupling.

Reference

[1] A.J. Dobbyn and P.J. Knowles, A comparative study of methods for describing non-adiabatic coupling: diabatic representation of the $^1\Sigma^+/^1\Pi$ HOH and HHO conical intersections, Mol. Phys., 91 (1997), 1107-1123.

[2] S.K. Gray, C. Petrongolo, K. Drukker, and G.C. Schatz, Quantum wave packet study of nonadiabatic effects in O (^{1}D) + H_2 →OH + H, J. Phys. Chem. A, 103 (1999), 9448-9459.

[3] S.K. Gray, G. G. Balint-Kurti, G.C. Schatz, J.J. Lin, X.H. Liu, S. Harich, and X.M. Yang, Probing the effect of the H_2 rotational state in O(^{1}D) + H_2 →OH + H: Theoretical dynamics including nonadiabatic

effects and a crossed molecular beam study, J. Chem. Phys., 113 (2000), 7330-7344.

[4] T.S. Chu, X. Zhang, and K.L. Han, A quantum wave-packet study of intersystem crossing effects in the O(^{3}P, ^{1}D) + H_2 reaction, J. Chem. Phys., 122 (2005), 214301.

[5] M.H. Alexander, E.J. Rackham, and D.E. Manolopoulos, Product multiplet branching in the O(^{1}D) + H_2 →OH($^2\Pi$) + H reaction, J. Chem. Phys., 121 (2004), 5221-5235.

[6] S. Rogers, D.S. Wang, A. Kuppermann, and S. Walch, Chemically accurate ab initio potential energy surfaces for the lowest ^{3}A' and ^{3}A'' electronically adiabatic states of O(^{3}P) + H_2, J. Phys. Chem. A, 104 (2000), 2308-2325.

[7] R. Schinke and W.A. Lester, Trajectory studies of O + H_2 reactions on fitted ab initio surfaces. II. Singlet case, J. Chem. Phys., 72 (1980), 3754-3766.

[8] J.N. Murrell and S. Carter, Approximate single-valued representations of multivalued potential-energy surfaces, J. Phys. Chem., 88 (1984), 4887-4891.

[9] T. Ho, T. Hollebeek, H. Rabitz, L.B. Harding and G.C. Schatz, A global H_2O potential energy surface for the reaction O(^{1}D) + H_2 →OH + H, J. Chem. Phys., 105 (1996), 10472-10486.

[10] S.Y. Lin and H. Guo, Adiabatic and Nonadiabatic State-to-State Quantum Dynamics for O (^{1}D) + H_2 ($X^1\Sigma_g^+$, v_i=j_i=0) → OH($^2\Pi$, v_f, j_f) + H(^{2}S) Reaction, J. Phys. Chem., A 113 (2009), 4285-4293.

[11] T. Takayanagi, Nonadiabatic quantum reactive scattering calculations for the O (^{1}D) + H_2, D_2, and HD reactions on the lowest three potential energy surfaces, J. Chem. Phys., 116 (2002), 2439-2446.

[12] J. Brandao and C.M.A. Rio, Double-valued potential energy surface for H_2O derived from accurate ab initio data and including long-range interactions, J. Chem. Phys., 119 (2003), 3148-3159.

[13] S. Garashchuk, V.A. Rassolov, and G.C. Schatz, Semiclassical nonadiabatic dynamics based on quantum trajectories for the O(^{3}P, ^{1}D) + H_2 system, J. Chem. Phys., 124 (2006), 244307.

[14] B. Li and K.L. Han, Mixed Quantum-Classical Study of Nonadiabatic Dynamics in the O (^{3}P, ^{1}D) + H_2 Reaction, J. Phys. Chem. A, 113 (2009), 10189-10195.

[15] R.A. Kendall, T.H. Dunning, and R.J. Harrison, Electron-affinities of the 1st-row atoms revisited - systematic basis-sets and wave-functions, J. Chem. Phys., 96 (1992), 6796-6806.

[16] H.J. Werner, P.J. Knowles, R.D. Amos, A. Bernhardsson, A. Berning, P. Celani, D.L. Cooper, M.J.O. Deegan, A.J. Dobbyn, and F. Eckert, University of Stuttgart, Germany/University of Birmingham, UK, 2002.

[17] T.S. Ho, T. Hollebeek, H. Rabitz, S. Der Chao, R.T. Skodje, A.S. Zyubin, and A.M. Mebel, A globally smooth ab initio potential surface of the 1 A ' state for the reaction S(^{1}D) + H_2, J. Chem. Phys., 116 (2002), 4124-4134.

[18] S. Manzhos, X.G. Wang, R.Dawes, and T. Carrington, A nested molecule-independent neural network approach for high-quality potential fits, J. Phys. Chem. A, 110 (2006), 5295-5304.

[19] G.G. Balint-Kurti, A.I. Gonzalez, E.M. Goldfield and S.K. Gray, Quantum reactive scattering of O(^{1}D) + H_2 and O(^{1}D) + HD, Faraday Discuss., 110 (1998), 169-183.